DIGITAL TWIN TEST-BENCH PERFORMANCE FOR MARINE DIESEL ENGINE APPLICATIONS

Dmytro Minchev [1]
Roman Varbanets [1]
Oleksandr Shumylo [1]
Vitalii Zalozh [2]
Nadiia Aleksandrovska [1]
Pavlo Bratchenko [1]
Thanh Hai Truong [3]

[1] Odesa National Maritime University, Odesa, Ukraine

[2] Danube Institute of the National University „Odesa Maritime Academy", Ukraine

[3] DPATET Research Group, Ho Chi Minh City University of Transport, Ho Chi Minh City, Viet Nam

* Corresponding author: *dmytro.minchev@nuos.edu.ua (D. Minchev)*

ABSTRACT

The application of Digital Twins is a promising solution for enhancing the efficiency of marine power plant operation, particularly their important components – marine internal combustion engines (ICE). This work presents the concept of applying a Performance Digital Twin for monitoring the technical condition and diagnosing malfunctions of marine ICE, along with its implementation on an experimental test-bench, based on a marine diesel-generator. The main principles of implementing this concept involve data transmission technologies, from the sensors installed on the engine to a server. The Digital Twin, also operating on the server, is used to automatically process the acquired experimental data, accumulate statistics, determine the current technical state of the engine, identify possible malfunctions, and make decisions regarding changes in operating programs. The core element of the Digital Twin is a mathematical model of the marine diesel engine's operating cycle. In its development, significant attention was devoted to refining the fuel combustion model, as the combustion processes significantly impact both the engine's fuel efficiency and the level of toxic emissions of exhaust gases. The enhanced model differs from the base model, by considering the variable value of the average droplets' diameter during fuel injection. This influence on fuel vapourisation, combustion, and the formation of toxic components is substantial, as shown. Using the example of calibrating the model to the test results of a diesel engine under 27 operating modes, it is demonstrated that the application of the improved combustion model allows better adjustment of the Digital Twin to experimental data, thus achieving a more accurate correspondence to a real engine.

Keywords: digital twin, combustion model, marine diesel engine, diagnostics

INTRODUCTION

Digital twin technology is a promising solution for current and future marine power plants. It could be used in various ways for various purposes: advanced control, monitoring and diagnostics, management and data analysis.

The idea of Digital Twin technology was originally developed for product lifecycle management issues, by M. Grieves in 2002, and subsequently refined by J. Vickers of NASA in 2010 [1]. It proved to be a very promising approach,

as the global market for Digital Twin products was valued at USD $3.8 billion in 2019 and is expected to reach USD $35.8 billion by 2025 [2].

The concept of Digital Twins has been experiencing rapid development in recent years. Today, Digital Twins are classified as the following types: Digital Twin Instance (DTI), Digital Twin Prototype (DTP) and Performance Digital Twin (PDT) [3]. However, all types of Digital Twins have common characteristics: high-fidelity, dynamic, self-evolving, identifiable, multiscale, metaphysical, and hierarchical [4], [5].

According to some specialists, the Digital Twin could be described as having the highest possible bidirectional integration level between the physical object and virtual model. In contrast, the Digital Shadow only reflects the state of the physical object while the Digital Model has no automatic interactions with the physical object [4]. Major areas for the implementation of Digital Twins are: smart cities and urban centers, freight logistics, medicine, engineering and automotive technologies.

A major area of Digital Twins applications is fault diagnostics and continuous monitoring of an object's tecnnical state. By combining Digital Twins with the deep transfer learning approach, accurate machine fault diagnosis could be provided, even with insufficient measured fault condition data [6]. The Digital Twin is continuously updated to generate possible fault conditions close to the actual asset and constructs the training data in the source domain for transfer learning. Digital Twin technology also can provide the visualisation of the monitoring process for the object being monitored, including 3D-visualisation and augmented reality technologies [7]. The very promising predictive maintenance method, based on Digital Twin, could be applicable in many areas and presents three unique characteristics: real-time perception, a high fidelity model and high confidence simulation prediction [8].

For a marine power plant and its components, Digital Twin could serve various purposes, among which are: prototyping and design, technical state monitoring and diagnostics, control and efficiency analysis, lifecycle management. It could also be a solution for environmental impact monitoring from shipping, which is one of the IMO goals with high priority [9]. Various components of marine power plants require monitoring [10], [11], while diesel engines remain one of the most important.

In terms of marine diesel engines, the most challenging factors for the successful implementation of Performance Digital Twin are: accurate engine operation simulation and enabling fast calculations. Obviously, for engine control tasks, it is necessary to provide 'real-time' engine operating process calculations [12], [13]. The ultimate goal should be defined as: engine operating cycle synthesis time equal to the actual engine operating cycle time. It is always a trade-off between calculation time and accuracy, which should be considered at the decision making stage of choosing an appropriate mathematical model for the Digital Twin core.

Engine manufacturers can potentially adopt high-fidelity Digital Twins for real-time engine control issues, as they have all the complete information about engine sub-systems and components. The heuristic-type model could be applied in this case [14]. In contrast, the monitoring systems with Digital Twins provided by external independent developers should have the characteristic of flexible tuning and adaptation, even in the absence of data.

One of the most critical things for the sufficient operation of Digital Twins is the correct prediction of the heat release process in the engine cylinder due to the fuel burning. Simulation of fuel combustion represents the toughest challenge, in terms of the development of the Digital Twin mathematical model, as the processes of fuel injection, atomisation, evaporation,

mixing with air and combustion are extremely complicated. Although some researchers reported the application of simplified combustion models, based on the Wiebe function [15], it has a huge limitation, in terms of predicting fuel timing and atomisation parameters for combustion processes.

This paper presents developments in the proven Razleitsev combustion model for marine diesel engines with Digital Twins and the research test-bench, based on the marine diesel-generator, which proves the concept. The research focuses on improvements in fuel evaporation and mixing prediction and its effect on further combustion and pollutant formation processes.

DIGITAL TWIN FOR ENGINE MONITORING AND CONTROL

A Digital Twin type of marine diesel engine serves the following purposes: monitoring of an engine's technical state, diagnostics of possible malfunctions, and control of the engine operating mode. For these purposes, the Digital Twin has to include the mathematical model of the engine operating cycle, which meets the requirements of accuracy and computational speed.

The diagram of the Digital Twin-based engine monitoring system is shown in Fig. 1. The engine is equipped with an array of sensors, allowing measurement of the engine's operating parameters. All of the sensors transfer the data to the set of controllers, which transmits the data to a Web Server via a Wi-Fi wireless connection.

The Web Server contains the Database, which stores the measured data, as well as the data generated by the Digital Twin. The Digital Twin autonomously takes data from the Database and runs the necessary calculations to compare the measured data with the predicted engine performance.

The visualisation of the actual engine operation and the predicted engine performance is provided in a pseudo real-time mode for educational and scientific purposes. Based on the comparison of the experimental and predicted engine performance, the Digital Twin provides diagnostic information related to the conditions of engine subsystems, such as: the turbocharging system, the fuel injection system and the gas distribution mechanism.

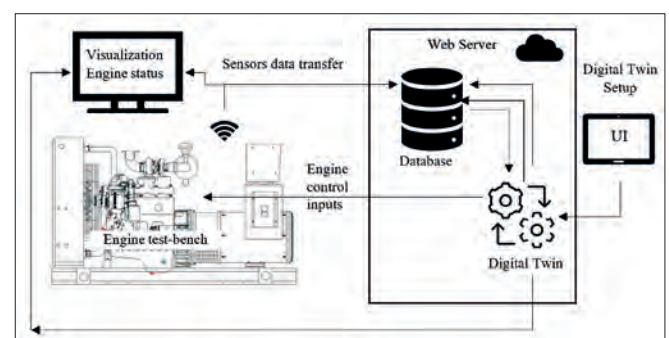The Digital Twin also has to set up the user interface before it can be used in an actual engine.

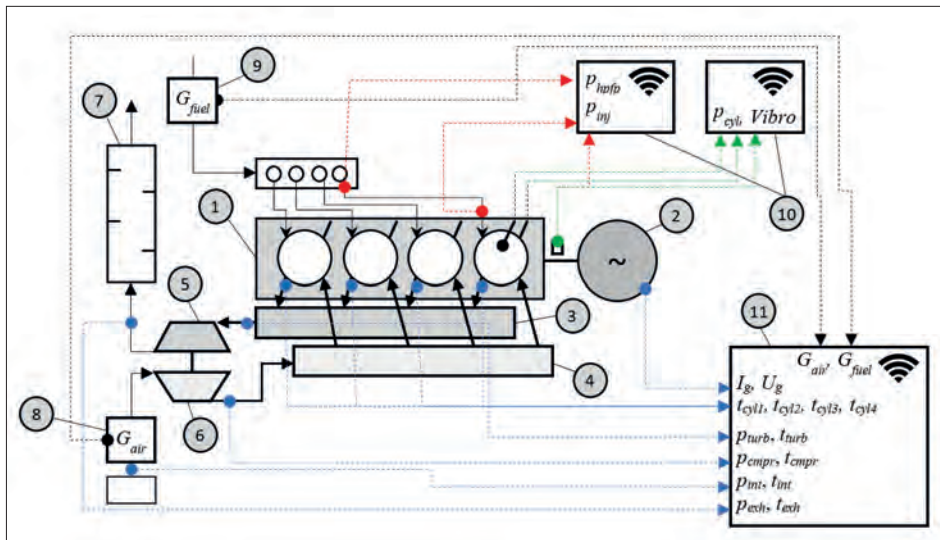*Fig. 1. Digital Twin application for engine control and monitoring issues.*

Fig. 2. Test-bench measuring points diagram:1 – engine; 2 – AC alternator; 3 – exhaust manifold; 4 – intake receiver; 5 – turbine; 6 – compressor; 7 – exhaust silencer; 8 – air mass flow meter; 9 – fuel mass flow meter; 10 – high-speed analogue-to-digital converters and transmitters; 11 – set of slow-speed analogueue-to-digital converters and transmitters.

We considered some detailed peculiarities of the concept using the actual test-bench as an example. The test-bench is based on the Weichai WP4C82-15 marine diesel-generator and was installed in the Odesa National Maritime University Laboratory.

The measuring device diagram is presented in Fig. 2 and it shows the measuring points and parameters. The measuring system can be considered as consisting of two sub-systems: 'static' and 'dynamic'. The former has low-speed parameters, which are measured as averages of the number of engine crankshaft revolutions, and the latter are high-speed parameters, which show the engine operating cycle as a function of the crank angle degree (the measuring step is 0.5-1.0 c.a.d.).

Static parameters include intake and exhaust system temperatures and pressures, engine power, air and fuel flow. The turbocharger speed is estimated by an acoustic method, as described in [16]. Dynamic parameters embrace in-cylinder pressure, pressures at the exit of the fuel injection pipe and before the fuel injector and the vibration sensor signal. The vibration sensor provides vibroacoustic data concerning fuel injection, and intake and exhaust valve timings [17], [18]. The obtained data is preprocessed using a special treatment for indicated diagrams analysis [19].

The database diagram, shown in Fig. 3, shows its basic structure and includes tables for both static and dynamic parameters.

The Digital Twin is based on the Blitz-PRO online service, providing simulations of both the static and transient operation of Internal Combustion Engines of various types [20]. The mathematical model of the engine's operating cycle is based on the two-zone quasi-steady approach for in-cylinder process synthesis, one-dimensional simulation of the intake and exhaust pipes processes, and advanced supercharger performance map treatment.

The important task of providing the closed-loop modelling of the operating process of a turbocharged engine is solved using the advanced characteristic maps of supercharging devices.
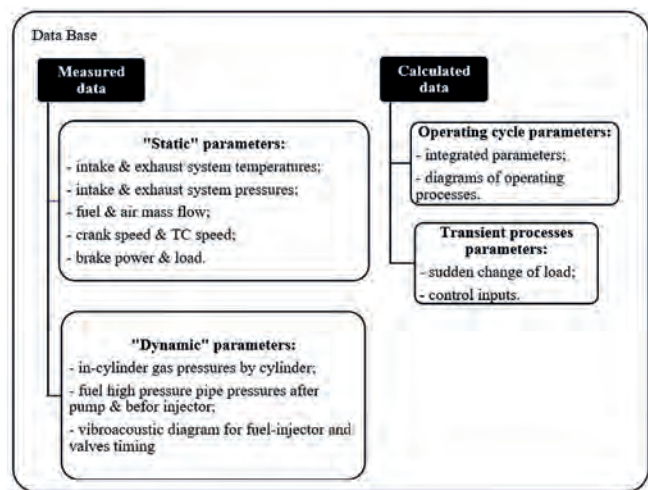

Fig. 3. Database structure.

Among other things, these maps allow for the consideration of phenomena such as compressor surge in a turbocharger [21].

The mathematical model of fuel combustion is based on the Razleitsev method for the equivalent fuel spray approach and the toxic emission estimation implements Zvonov's method of burned zone gas composition prediction. As the fuel combustion processes have a significant impact on the performance parameters of the engine and the level of toxic emmisions in the exhaust gases, as well as the fact that these processes have an inherently complex physicochemical nature, one of the most important components for the mathematical model of a Digital Twin is a precise fuel combustion model.

As the fuel combustion depends greatly on the movement of fuel spray, the injection rate diagrams, fuel atomisation and in-cylinder air motion, the application of a complex combustion model is challenging; this type of information is hardly achievable at engine operating conditions. From this point of view, the combustion model should be simple enough to set up and apply to practical power plants and accurate enough to correctly replicate engine performance.

IMPROVEMENTS IN FUEL COMBUSTION MODEL

The fuel combustion model for diesel engines was proposed for the equivalent spray approach by Razletsev in 1980 [22], and further developed in 1992 [23], to account for the peculiarities of fuel jet motion with a detailed mechanism of interaction between the fuel flame and the combustion chamber walls. Subsequently, Razletsev's model was slightly improved by Kuleshov [24] and implemented in commercial software tools for the calculation of engine operating processes.

Razletsev's method involves a sequential and interconnected consideration of the fuel injection, evaporation, mixture formation, and fuel combustion using fundamental laws of physics and chemical kinetics.

The characteristics of fuel injection are determined using experimental or statistical data. The basic Razletsev method assumes single injection events but it can be adopted for multiple injections, as we will show later. The movement of fuel sprays and their atomisation is determined using criteria equations proposed by Lyishevsky.

$$
\begin{cases}
l_a = 1.22 \cdot l_c \cdot \rho^{-0.5} \Im_g^{-0.35} \cdot \Im^{0.35} e^{-0.2(\frac{\tau}{\tau_c})} \; ; \\
l_b = \sqrt{d_{inj.holes} u_0 We^{0.21} M^{0.16} / (3\sqrt{2}\overline{\rho}) \tau^{0.5}} \; ; \\
l_c = 8.85 d_{inj.holes} We^{0.25} M^{0.4} \overline{\rho}^{-0.6} \; ;
\end{cases}
\tag{1}
$$

$$
d_{32} = 10^6 E_c d_{inj.holes} \frac{M^{0.0733}}{(\overline{\rho} We)^{0.266}} \; ;
\tag{2}
$$

$$
M = \frac{\mu_{fuel}^2}{d_{inj.holes} \rho_{fuel} \sigma_{fuel}} \; ; \quad \overline{\rho} = \frac{\rho_c}{\rho_{fuel}} \; ;
$$

$$
We = \frac{u_{inj}^2 d_{inj.holes} \rho_{fuel}}{\sigma_{fuel}} \; ; \quad \Im = \frac{\tau^2 \sigma_{fuel}}{d_{inj.holes}^3 \rho_{fuel}} \; ;
$$

where l_a, l_b and l_c are the spray length development at the initial stage, the main stage of injection and at the end of the initial stage; τ and τ_c are time moments from injection start and from injection start to the end of the initial stage of injection; μ_{fuel}, ρ_{fuel}, and σ_{fuel} are the dynamic viscosity, specific gravity and surface tension of the fuel; E_c is a coefficient; and $d_{inj.holes}$ is the nozzle hole diameter.

Fuel atomisation is characterised with the Sauter diameter of fuel droplets d_{32}, which is the ratio of the total volume of fuel drops to their combined surface area. For simplification reasons the value d_{32} was considered to be constant by Razletsev and equal to the average for the injection period [22], [23].

To calculate the fuel evaporation, a modification of Sreznevsky law for the evaporation of an individual droplet is used. To determine the fraction of fuel evaporated at a given moment in time, integration is performed for all fuel portions injected up until that moment:

$$
\frac{d\sigma_{ev}}{d\varphi} = \int_{\varphi_{inj.start}}^{\varphi} \frac{3}{2}\chi_{wall} b_{ev}\left(1 - \chi_{wall} b_{ev} \frac{\varphi - \varphi_{inj.start}}{6n}\right)^{0.5}\left[\frac{d\sigma}{d\varphi}\right] d\varphi,
\tag{3}
$$

where σ_{ev} is the evaporated portion of the fuel; $d\sigma/d\varphi$ is the relative injection rate; b_{ev} is the evaporation constant; and χ_{wall}

is the reduction in the evaporation rate which occurs when fuel interacts with the walls.

It should be noted that Razletsev and his followers, instead of using the accurate solution mentioned above, used a simplified equation, **assuming a constant injection rate** over the injection process time and equal to the average value:

$$
\frac{d\sigma_{ev}}{d\varphi} = \frac{1}{\varphi_{inj}} \chi\left([1 - b_{ev}(\varphi - \varphi_{inj})]^{3/2} - [1 - b_{ev}]^{3/2}\right).
\tag{4}
$$

The use of the simplified equation lead to a significant error in the calculation results, as shown in Fig. 4. For nonlinear injector rate profiles, the cumulative error of the evaporated fuel share could exceed 20% and so the application of the accurate solution is important.
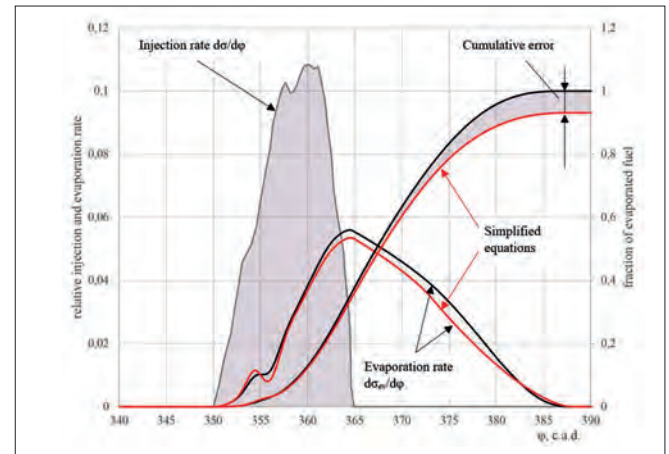

Fig. 4. Comparison of fuel injection rate diagrams calculated using simplified and accurate equations

The fuel evaporation constant is dependent on the average diameter of the fuel spray droplets d_{32} and can be calculated using the following expression:

$$
b_{ev} = Y \frac{10^{12}}{d_{32}^2} \frac{1}{p_c} ,
\tag{5}
$$

where Y is the correction factor; p_c is the end pressure of the compression process; and m_Y is the exponent of the evaporation function.

According to Razletsev's recommendations, the correction factor Y can be calculated using the following expression:

$$
Y = \left(\frac{n_{crank}}{1000}\right)^{m_Y} ,
\tag{6}
$$

where m_Y is the exponent of the evaporation correcting function.

Typically, m_Y is chosen within the range 0.65-1.00. However, if the crankshaft rotational speed of the engine is below 1000 rpm, the value of m_Y can be selected within the range 0.35-0.70. These values allow for appropriate adjustments in the evaporation function, to account for different engine operating conditions.

Kuleshov proposed a more complex expression for the function Y:

$$
Y = 0.372 \cdot 10^{-9}(18 + y_s + y_{rpm}) y H_y^{0.35} d_{32}^{-1.5},
\tag{7}
$$

where $y_s = f(S)$ is the scaling factor dependent on the piston stroke S; $y_{rpm} = f(n_{crank})$ is the correction coefficient dependent on the crankshaft rotational speed ncrank; Hy is the corrected swirl number; and y is an empirical coefficient ranging from 5-35.

This more comprehensive expression for the function Y considers additional factors, such as piston stroke, crankshaft rotational speed, and the corrected swirl number, to provide a more accurate estimation of the evaporation constant. From the given expression, we can conclude that the evaporation constant is variable during fuel injection and depends on the average diameter of the droplets.

The relative reduction in the evaporation rate when the fuel sprays come into contact with the combustion chamber walls, according to the original methodology [22], can be calculated using the following equation:

$$\chi_{wall} = 1 - \left(\frac{1-\chi_0}{0.485}\right) \cdot 0.707 \left(\frac{\varphi-\varphi_{wall}}{\varphi_{fr}}\right) \cdot \frac{2}{\sqrt{\pi}} e^{-0.5\left(\frac{\varphi-\varphi_{wall}}{\varphi_{fr}}\right)^2} ;$$

$$\varphi_{fr} = A_{st} \cdot 2\varphi_{wall} \frac{\bar{\rho}^{0.5} We^{0.32}}{M^{0.07}}, \qquad (8)$$

where φ_{wall} is the moment when the spray reaches the combustion chamber wall; χ_0 is the minimum value of the reduction coefficient of the evaporation rate; φ_{fr} is the duration of the interaction between the spray and the combustion chamber walls; and A_{st} is the coefficient in the formula for calculating the cone angle of the fuel spray.

To calculate the ignition delay period, a modified Tolstov equation is used:

$$\tau_i = B_0(1- k_n n_{crank}) \sqrt{\frac{p_{cyl}^{in.j.start}}{T_{cyl}^{in.j.start}}} \, e^{\frac{E_a}{RT_{cyl}^{in.j.start}}} \frac{70}{25+CN}, \qquad (9)$$

where B_0 and k_n are coefficients; $p_{cyl}^{in.j.start}$ and $T_{cyl}^{in.j.start}$ are the pressure and temperature at the beginning of compression; and E_a and CN are the activation energy and cetane number of the fuel.

In a further development, a more advanced model of the fuel spray was proposed, which includes the following seven characteristic zones [23]: dense axial core, dense front jet, rarefied jet envelopee, conical axial core of the boundary flow, boundary flow core on the piston surface (head, cylinder liner), and rarefied boundary flow envelope. For each of these characteristic zones, the fuel evaporation constant is calculated using individual equations.

The application of a more advanced model of fuel sprays complicates the combustion model tuning process and requires accurate information about the geometry of the combustion chamber and fuel injector, which is not always available.

During the calculation of heat release, the following processes are considered separately: combustion of the air-fuel mixture formed during the ignition delay period, diffusion combustion in the fuel supply region, and post-injection fuel burning after the end of injection. The transition between equations for each stage occurs at specific time points: when $x = \sigma_i$ from the equations for the first stage to the equations for the second stage, and when $\varphi = \varphi_{inj.end} + \Delta\varphi_{k.ext}$ from the equations for the second stage to the equations for the third stage. The continuation of using the equations for the second stage after the end of injection

is possible for a period of $\Delta\varphi_{k.ext}$ by setting the parameters $\Delta\varphi_k$ and $\Delta\tau_k$.

Typically, for the external characteristic, $\Delta\varphi_k = 0$, reaching values of 5-12 in idle modes, while $\Delta\tau_k$ is recommended to be selected in the range of 0.3-0.8 for direct injection and 0.5-0.9 for split combustion chambers. The basic system of equations is as follows:

$$\frac{dx}{d\varphi} = \begin{cases} \frac{1}{6n}\left(\left(P_0 + 6n_{crank}\frac{d\sigma_{ev}}{d\varphi}\right)\bigg/\left(1 + A_1\left(P_0 + 6n_{crank}\frac{d\sigma_{ev}}{d\varphi}\right)\right)\right)\bigg|_{x=0}^{x=\sigma_i} ; \\ \frac{1}{6n}\left(P_2 + 6n_{crank}\frac{d\sigma_{ev}}{d\varphi}\right)\bigg/\left(1 + A_1 6n_{crank}\frac{d\sigma_{ev}}{d\varphi}\right)\bigg|_{\sigma=\sigma_i}^{\varphi=\varphi_{inj.end}+\Delta\varphi_{k.ext}} ; \\ \frac{1}{6n} A_3 \frac{\xi_{a.c}\alpha}{x}(1 - \Delta_{U.F} - x)x)\bigg|_{\varphi=\varphi_{inj.end}+\Delta\varphi_{k.ext}}^{\varphi=\varphi_{comb.end}} . \end{cases}$$

$$(10)$$

where σ_i is the fraction of fuel supplied during the ignition delay period; $\varphi_{inj.end}$ is the end of injection moment; $\Delta\varphi_{k.ext}$ is the extended period of applying the second equation; $\Delta\varphi_{comb.end}$ is the end of the combustion process; $\xi_{a.c}$ is the air utilisation function; and $\Delta_{U.F}$ is the unburned fuel fraction.

Functions P_0, P_2, A_0, and A_2 are determined according to the equations:

$$\begin{cases} P_0 = \frac{A_0 q_{fuel}(\sigma_{ev}-x_0)}{V(\varphi_{comb.start})}(b_0\,\sigma_{ev} + x_0) ; \\ P_2 = \frac{A_2 q_{fuel}(\alpha-x)}{V_c}(\sigma_{ev} - x); \end{cases}$$

$$(11)$$

$$\begin{cases} A_0 = a_0\,(n \cdot H)^{m_{comb}} ; \\ A_1 = a_1\,(n \cdot H)^{m_{comb}} ; \\ A_2 = a_2\,(n \cdot H)^{m_{comb}} , \end{cases}$$

$$(12)$$

where H is a swirl number; and a_0, a_1, a_2, b_0, and m_{comb} are adjustable coefficients.
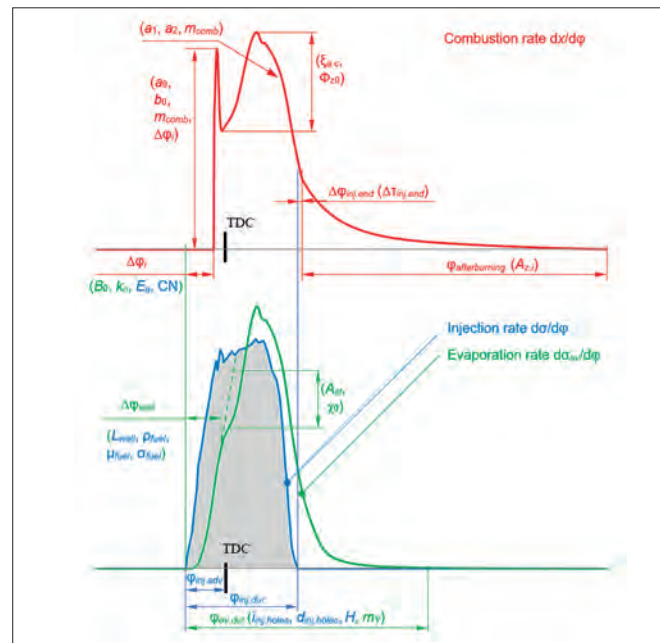

Fig. 5. The relationship between fuel injection, fuel vapourisation processes, and fuel combustion for the Razleytsev model, along with the model tuning parameters for a single injection case.

Engine type	$a_0 \cdot 10^{-3}$	$a_1 \cdot 10^2$	a_2	b_0	m_{comb}	H	m_Y
$n = 50...250$ rpm, two-stroke	5...12	5...10	10...15	0.1...0.2	0.6...0.8	1.5...3	0.30...0.65
$n = 400...750$ rpm, four-stroke	8...15	4...9	8...13	0.05...0.15	0.5...0.7	1...1.1	0.45...0.7
$n = 750...1500$ rpm, two-stroke	10...40	3...7	4...8	0.05...0.1	0.5...0.7	1...1.2	0.5...0.75
$n > 1500$ rpm, two-stroke	15...30	3...6	3...7	0.04...0.08	0.6...0.8	1.2...2	0.5...0.9

As seen from the given system of equations, the first and second stages of the combustion process are significantly influenced by fuel vapourisation rate and mixture formation, while the fuel post-injection stage is determined by the air utilisation function in the engine cylinder $\zeta_{a.c}$:

$$\zeta_{a.c} = 1 - 1.46(1 - \zeta_{a.c0}) \frac{\Phi_z}{\Phi_{z0}} \frac{2}{\sqrt{\pi}} e^{-0.5\left(\frac{\Phi_z}{\Phi_{z0}}\right)^2} , \qquad \textbf{(13)}$$

where Φ_z is the relative combustion duration; and $\zeta_{a.c0}$ and Φ_{z0} are the coordinates of the minimum of the function $\zeta_{a.c} = \zeta_{a.c}(\Phi_{z0})$.

Table 1 provides typical values of the coefficients in the fuel combustion model equations for different types of engines, while Fig. 5 illustrates the influence of various tuning parameters on the characteristics of heat release.

CONSIDERING VARIABLE FUEL DROPLETS SIZE DURING INJECTION

As previously mentioned, Razleitsev used the average value of the fuel droplet diameter d_{32} to predict fuel evaporation and considered it to be constant during injection. In his latest studies, Kuleshov considered variable fuel droplet size for the ignition delay period [24], [25]. Obviously, this means that the fuel evaporation constant b_{ev}, as well as the correction factor Y, are also constant in the evaporation process. To examine the applicability of simplified equations, consider Fig. 6-8, which show the calculated fuel evaporation diagrams for two cases: assuming a variable fuel droplets size across the injection process and using the constant value of d_{32} averaged for the injection period (d_{32} = const). As shown, assuming the variable fuel droplets diameter makes a significant impact on fuel the evaporation diagrams, which causes a further influence on fuel combustion and in-cylinder pressure build-up.
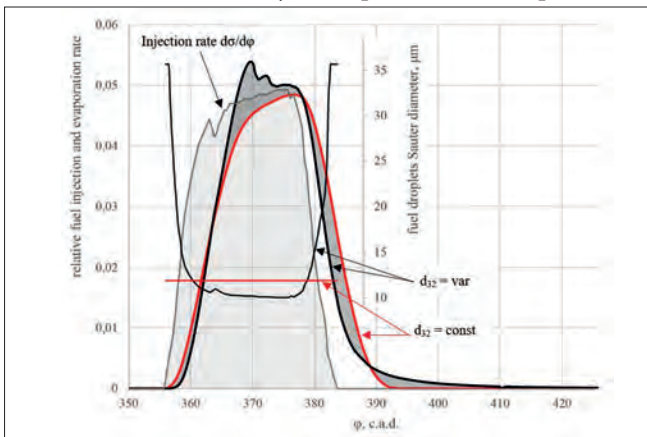

Fig. 6. Calculated diagrams of fuel evaporation rate. Medium-speed diesel engine, MCR.
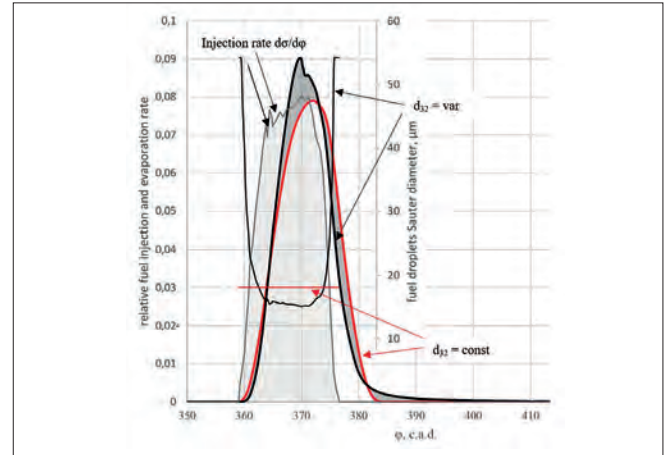

Fig. 7. Calculated diagrams of fuel evaporation rate. Medium-speed diesel engine, 40% of MCR.
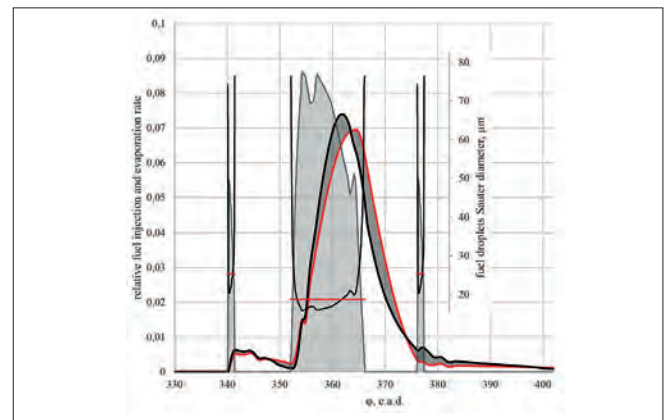

Fig. 8. Calculated diagrams of fuel evaporation rate. High-speed diesel engine, triple injection, part load.

Fuel combustion processes contribute to the emission of toxic compounds in the exhaust gases of marine diesel engines. These emissions primarily consist of CO, soot (and other particulate matter), SO_x, and NO_x. Accurate prediction of the buildup of toxic emissions is crucial for the application of engine Digital Twins.

CONSIDERING TOXIC EMISSION FORMATION IN THE COMBUSTION PROCESSES

In order to predict the gas composition in different zones, a two-zone combustion model is employed. This model separates the fresh charge zone from the burned gases zone. The composition of the burned gases is determined using Professor Zvonov's method, which assumes an 18-component mixture consisting of O, O_2, O_3, H, H_2, OH, H_2O, C, CO, CO_2, CH_4, N, N_2, NO, NO_2, NH_3, HNO_3, and HCN.

The calculation of NO_x concentration in the exhaust gas is based on the Zeldovich mechanism for 'thermal' nitric oxide (NO). This mechanism involves a series of three equations.

The first equation is the most important, in terms of total NO formation kinetics. The equation for NO kinetics can be expressed as:

$$\frac{d[NO]}{d\tau} = K_{1p}[N_2][O] - K_{1r}[NO][N] - K_{2r}[NO][O] +$$
$$K_{3p}[N][OH] - K_{3r}[NO][H],$$

where the square brackets '[ ]' express the volumetric concentration of the corresponding matter, and K_{1p}, K_{1r}, K_{2p}, K_{2r}, K_{3p}, and K_{3r} are constants for direct and reverse chemical reactions.

The NO formation kinetic equation incorporates the first and second equations, based on Zvonov's approach:

$$\frac{d[NO]}{d\tau} = \frac{2K_{1p}[N_2][O]}{1 + \frac{K_{1r}[NO]}{K_{2p}[O_2]}}\left(1 - \frac{[NO]^2}{K_4[O_2][N_2]}\right); \quad K_4 = \frac{K_{1p}K_{2p}}{K_{1r}K_{2r}};$$

(14)

It should be noted that $K_4[O_2][N_2] = [NO]_{eq}$ is the equilibrium concentration of NO.

The conversion of the equation into volumetric fraction units gives:

$$\frac{d[NO]}{d\tau} = \frac{p}{RT_{burned}}\frac{2K_{1p}[N_2][O]}{1 + \frac{K_{1r}[NO]}{K_{2p}[O_2]}}\left(1 - \left(\frac{[NO]}{[NO]_{eq}}\right)^2\right),$$

(15)

where p is the pressure in the cylinder (bar); $R = 8.3144$ J/(mole·K) is the gas constant; and T_{burned} is the temperature of the burned gases.

The Arrhenius Law equations are used to calculate reaction rate constants:

$$K = AT^B \exp\left(-\frac{E_a}{RT}\right),$$

(16)

where A and B are empirical coefficients; and E_a is the activation energy.

For high-speed engines, the final concentration of CO in exhaust gases is estimated as an equivalent concentration at the combustion finish point. For medium-speed and low-speed diesel engines, the following kinetic equation is used:

$$\frac{d[CO]}{d\tau} = K_{1C}[CO][OH],$$

(17)

where $K_{1C} = 7.1 \cdot 10^{12} \cdot e^{-32200RT}$ is the reaction constant; and $[CO]$ and $[OH]$ are the corresponding CO and OH concentrations.

Calculation of the formation of particulate matter in diesel engines is performed using Razlejtsev's approach. The equation for the instantaneous volumetric soot concentration rate is as follows:

$$\frac{d[C]}{d\tau} = \left(\frac{d[C]}{d\tau}\right)_{kin} + \left(\frac{d[C]}{d\tau}\right)_{pol} - \left(\frac{d[C]}{d\tau}\right)_{burn} - \left(\frac{d[C]}{d\tau}\right)_{vol}.$$

(18)

The components of this equation are:
- the kinetic soot formation rate (in the flame)
$\left(\frac{d[C]}{d\tau}\right)_{kin} = B_{1S}\frac{q_{fuel}}{V}\frac{dx}{dt};$
- the core polymerisation of fuel droplets rate during fuel injection:

$$\left(\frac{d[C]}{d\tau}\right)_{pol} = B'_{2s}\delta_d\frac{q_{fuel}}{V}\frac{1 - exp\left(-\left(\frac{\sqrt{K_{ev}(\tau - \tau_{inj.start})}}{d_{32}}\right)^{n_{disp}}\right)}{\tau_{inj}},$$

and after fuel injection ends:

$$\left(\frac{d[C]}{d\tau}\right)_{pol} = B''_{2s}\delta_d(1 - x_{inj.end})\frac{n_{disp}q_{fuel}}{2V(\tau - \tau_{inj.end})}$$

$$\left(\frac{\sqrt{K_{ev}(\tau - \tau_{inj.start})}}{d_{32}}\right)^{n_{disp}}\frac{1 - e^{-\left(\frac{\sqrt{K_{ev}(\tau - \tau_{inj.start})}}{d_{32}}\right)^{n_{disp}}}}{\tau_{inj}};$$

- the soot particles burning rate:
$\left(\frac{d[C]}{d\tau}\right)_{burn} = B_{3S}k_{O_2}\sqrt{n} \cdot p \cdot [C];$
- and the change in soot concentration rate due to cylinder volume change:
$\left(\frac{d[C]}{d\tau}\right)_{vol} = B_{4S}\frac{6n}{V}\frac{dV}{d\phi}.$

In the above equations B_{1s}, B'_{2s}, B''_{2s}, B_{3s}, and B_{4s} are empiric coefficients; δ_d is the droplet core size; K_{ev} is the evaporation constant; $\tau_{inj.start}$ and $\tau_{inj.end}$ are moments of time for injection start and injection end; $x_{inj.end}$ is the burned fuel fraction for the moment of injection end; n_{disp} is the distibution constant to consider fuel injection uniformity; k_{0_2} is the oxidation coefficient; and $[C]$ is the volumetric soot concentration.
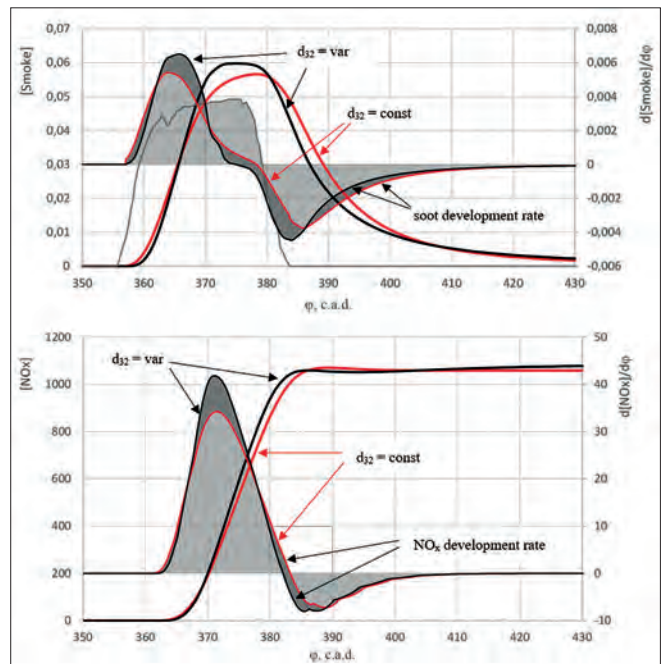

Fig. 9. Soot concentration and nitrogen oxide development in the cylinder. Medium-speed engine, MCR.

The oxidation coefficient is considered using following equation:

$$k_{O_2} = 1.8 \left(1 - \left(1 - (1 - \alpha)\frac{L_0}{M_2}\right) x\right), \quad \text{(19)}$$

where L_0 is the stoichiometric amount of air (in kmole per 1 kg of fuel); and M_2 is the amount of combustion products (in kmole per 1 kg of fuel).

The influence of the variable diameter of fuel droplets, considering during the development of toxic emmissions, is illustrated in Fig. 9.

DISCUSSION

Therefore, it can be concluded that, the variable size of fuel droplets during injection is significant in the provided combustion model, as it not only substantially affects the processes of vapourisation, mixture formation, and combustion, but also the formation of toxic emissions, primarily nitrogen oxides and particulate matter. The proposed improvements in the mathematical model allow for a more accurate calibration with experimental data and, importantly for its Digital Twin application, do not lead to an increase in calculation time.

As an example, consider the calibration of a Digital Twin for a high-speed diesel engine with a cylinder diameter/stroke of 120/120 mm, using the results of its comprehensive testing under 27 operating modes, including the determination of emissions of key pollutants (nitrogen oxides) and smoke opacity of the exhaust gases.

Table 2 illustrates the values of relative errors in determining the specific indicated fuel consumption b_{ii}, concentrations of nitrogen oxides [NOx], and smoke opacity [Smoke]. Consideration of variable fuel droplet size during injection helped to obtain better cumulative accuracy, calculated with the equation:

$$\delta_{\Sigma} = \sqrt{\frac{\Sigma \delta_i^2}{N}}, \quad \text{(20)}$$

where $N = 27$ (the total number of measurements).

Table 2 shows that consideration of fuel droplet size variation helped to simultaneously increase the accuracy of the prediction of b_i – from $\delta_{\Sigma} = 5.7\%$ to $\delta_{\Sigma} = 5.1\%$, [NOx] – from $\delta_{\Sigma} = 6.2\%$ to $\delta_{\Sigma} = 3.2\%$ and [Smoke] from $\delta_{\Sigma} = 41.6\%$ to $\delta_{\Sigma} = 17.8\%$.

However, it is necessary to acknowledge that the proposed refinement of the combustion model, which is thoroughly grounded from a theoretical standpoint, presents certain pragmatic challenges. It becomes evident that, in order to optimally harness the enhanced capabilities of the model, the characteristics of the fuel injection (in the form of multi-parameter functions denoted as $d\sigma/d\varphi = f(\text{rpm, bmep})$) are required, at the very least. The procurement of such data necessitates the execution of intricate and dedicated experimental investigations, typically carried out on specialised test-benches.

It is essential to consider that the mere existence of such dependencies under actual operating conditions is insufficient, as these relationships are derived for the proper state of the fuel system: the high-pressure fuel pump, high-pressure pipes, and fuel injector.

Thus, it is necessary to be able to assess the characteristics of fuel injection during the engine's operation. To achieve this, use of the following data is proposed:

- In the case of a research engine, sensors for fuel pressure are installed after the high-pressure fuel pump and directly in front of the injector, as shown in Fig. 2. These sensors allow for obtaining pressure diagrams at the corresponding points, as well as a vibroacoustic sensor.
- For engines operating within a marine power plant, if the installation of pressure sensors is not provided for by the design, a vibroacoustic sensor is exclusively used, which enables the acquisition of the moments of the beginning and end of fuel injection [17].

The data obtained from the sensors allow for obtaining the necessary characteristics of fuel injection and, importantly, taking into account their changes due to wear or malfunctions of the fuel apparatus. A detailed review of the algorithms and results of similar data processing requires a separate publication and represents a prospect for further research.

Specifically indicated fuel consumption biNitrogen oxide content at exhaust [NOx]Particulate matter content at exhaust [Smoke]

CONCLUSIONS

Digital Twin technology represents a promising direction for enhancing the operational efficiency of marine internal combustion engines. The advanced systems for monitoring the technical conditions and diagnosing engine malfunctions can be developed, complying with the principles and requirements of the fourth industrial revolution for modern transportation systems. The performance-type Digital Twin, as the core element of these systems, uses the data from engine sensors to predict the virtual operating cycle, which gives additional information about engine parameters and helps to estimate the efficiency of the engine and detect possible malfunctions.

Technically, the monitoring system includes the server with the database for the engine operating parameters, transmitted from the set of sensors. The data include slow-speed 'static' and high-speed 'dynamic' parameters. The Digital Twin uses the database in autonomous mode and is also capable of providing the malfunctions alarm or control inputs.

When developing a Digital Twin for an internal combustion engine, it is important to reliably and accurately calculate the development of the fuel combustion processes, as they significantly impact both the engine's efficiency and the level of toxic emissions in exhaust gases. Considering the variation in fuel droplet diameter during the injection process, allows for a substantial improvement in the accuracy of engine modelling using the Digital Twin, as is shown for the set of 27 operational points of the high-speed diesel engine.

Tab. 2. Relative accuracy of Digital Twin predicted diesel engine parameters

Specifically indicated fuel consumption b_i

Crank speed	Ignition advance	d_{32} = const		δ_Σ=5.7%	d_{32} = var		δ_Σ=5.1%
		40% load	70% load	100% load	40% load	70% load	100% load
1000	10	14.1%	2.8%	−0.7%	11.8%	1.2%	−1.4%
	13	14.9%	8.6%	5.9%	13.3%	7.3%	6.0%
	18	7.7%	4.5%	3.6%	6.8%	3.9%	3.2%
1400	10	3.5%	1.2%	−0.1%	1.8%	−0.4%	−1.5%
	13	9.5%	6.6%	2.0%	7.9%	5.3%	1.1%
	18	2.7%	2.7%	3.6%	2.0%	2.1%	3.4%
2200	10	−2.8%	−3.3%	0.9%	−4.5%	−4.5%	−1.7%
	13	1.6%	−1.7%	−2.6%	0.4%	−2.4%	−3.0%
	18	−4.2%	−2.6%	−0.8%	4.7%	−2.8%	−2.3%

Nitrogen oxide content at exhaust $[NO_x]$

Crank speed	Ignition advance	d_{32} = const		δ_Σ=6.2%	d_{32} = var		δ_Σ=3.2%
1000	10	−3.6%	−1.6%	−1.9%	1.7%	1.5%	1.6%
	13	−2.6%	0.4%	0.5%	−0.8%	−1.3%	−0.8%
	18	2.3%	1.4%	10.9%	−0.8%	−2.5%	3.2%
1400	10	−6.6%	3.7%	2.1%	−6.1%	−1.3%	1.3%
	13	−2.2%	0.4%	−1.0%	1.3%	−0.2%	−1.0%
	18	−0.9%	0.8%	−6.1%	0.9%	−3.6%	−2.9%
2200	10	11.1%	21.2%	−7.6%	−10.0%	4.5%	−6.4%
	13	−3.1%	1.8%	−3.3%	−2.0%	−1.3%	−1.0%
	18	10.6%	−3.0%	−0.2%	3.6%	−0.4%	−0.3%

Particulate matter content at exhaust [Smoke]

Crank speed	Ignition advance	d_{32} = const		δ_Σ=41.6%	d_{32} = var		δ_Σ=17.8%
1000	10	−12.6%	−1.9%	−6.9%	−23.8%	−1.3%	−4.2%
	13	13.9%	0.0%	−2.3%	0.0%	−0.1%	0.9%
	18	33.7%	14.2%	41.8%	12.6%	15.7%	43.7%
1400	10	−12.4%	7.5%	3.4%	−24.4%	5.0%	7.9%
	13	−8.6%	23.4%	−15.2%	−21.2%	25.1%	−10.6%
	18	10.2%	17.2%	11.9%	0.1%	18.6%	15.6%
2200	10	−24.5%	0.7%	−4.4%	−33.7%	−7.9%	−4.7%
	13	−20.6%	−2.9%	3.8%	−31.6%	−11.0%	1.1%
	18	−16.1%	−11.6%	3.7%	−24.3%	−15.6%	1.1%

However, for the successful utilisation of the additional capabilities inherent to the fuel combustion model, it is necessary to have the ability to conduct an evaluation of fuel injection characteristics during engine operation. This is proposed to be accomplished through the use of vibroacoustic sensors and, where feasible, pressure sensors within the fuel system, and represents the direction of future research.

REFERENCES

1. M. Grieves and J. Vickers, "Digital twin: Mitigating unpredictable, undesirable emergent behavior in complex systems," Transdisciplinary perspectives on complex systems: New findings and approaches. 2017, pp. 85-113, https://www.researchgate.net/profile/Michael-Grieves/

publication/306223791_Digital_Twin_Mitigating_
Unpredictable_Undesirable_Emergent_Behavior_in_
Complex_Systems/links/5aa54e1ea6fdccd544bc386f/
Digital-Twin-Mitigating-Unpredictable-Undesirable-
Emerge.

2. S. Evans, C. Savian, A. Burns and C. Cooper, "Digital Twins for the Built Environment: An Introduction to the Opportunities," Built Environmental News. 2019, https://www.theiet.org/media/8762/digital-twins-for-the-built-environment.pdf.

3. D. Botín-Sanabria, A.-S. Mihaita, R. Peimbert-García, M. Ramírez-Moreno, R. Ramírez-Mendoza and J. Lozoya-Santos, "Digital Twin Technology Challenges and Applications: A Comprehensive Review," Remote Sensing. 2022, vol. 14(6), no. 1335, doi: 10.3390/rs14061335.

4. M. Singh, E. Fuenmayor, E. Hinchy, Y. Qiao, N. Murray and D. Devine, "Digital Twin: Origin to Future," Appl. Syst. Innov. 2021, vol. 4, no. 36, doi: 10.3390/asi4020036.

5. L. Li, S. Aslam, A. Wileman and S. Perinpanayagam, "Digital Twin in Aerospace Industry: A Gentle Introduction," IEEE Access. 2022, vol. 10, pp. 9543-9562, doi: 10.1109/ACCESS.2021.3136458.

6. M. Xia, H. Shao, D. Williams, S. Lu, L. Shu and C.W. de Silva, "Intelligent fault diagnosis of machinery using digital twin-assisted deep transfer learning," Reliability Engineering & System Safety. 2021, vol. 215, doi:10.1016/j.ress.2021.107938.

7. S. Choi, J. Woo, J. Kim and J. Lee, "Digital Twin-Based Integrated Monitoring System: Korean Application Cases," Sensors. 2022, vol. 22, no. 5450, doi: 10.3390/s22145450.

8. D. Zhong, Z. Xia, Y. Zhu and J. Duan, "Overview of predictive maintenance based on digital twin technology," Heliyon. 2023, vol. 9, no. 4, doi: 10.1016/j.heliyon.2023.e14534.

9. A.T. Hoang, A.M. Foley, S. Nižetić, Z. Huang, H.C. Ong, A.I. Ölçer, V.V. Pham and X.P. Nguyen, "Energy-related approach for reduction of CO2 emissions: A critical strategy on the port-to-ship pathway," Journal of Cleaner Production. 2022, vol. 355, doi:10.1016/j.jclepro.2022.131772.

10. O. Melnyk, O. Sagaydak, O. Shumylo and O. Lohinov, "Modern Aspects of Ship Ballast Water Management and Measures to Enhance the Ecological Safety of Shipping," in Systems, Decision and Control in Energy V. Studies in Systems, Decision and Control, Springer ed. 2023, vol. 481, Cham, doi: 10.1007/978-3-031-35088-7_39.

11. O. Onishchenko, A. Bukaros, O. Melnyk, V. Yarovenko, A. Voloshyn and O. Lohinov, "Ship Refrigeration System Operating Cycle Efficiency Assessment and Identification of Ways to Reduce Energy Consumption of Maritime Transport," in Systems, Decision and Control in Energy V. Studies in Systems, Decision and Control, 2023, vol 481. Springer, Cham., doi: 10.1007/978-3-031-35088-7_36.

12. S. Hautala, M. Mikulski, E. Söderäng, X. Storm and S. Niemi, "Toward a digital twin of a mid-speed marine engine: From detailed 1D engine model to real-time implementation on a target platform," International Journal of Engine Research. 2022, doi: 10.1177/14680874221106168.

13. S. Stoumpos, G. Theotokatos, C. Mavrelos and E. Boulougouris, "Towards Marine Dual Fuel Engines Digital Twins — Integrated Modelling of Thermodynamic Processes and Control System Functions," J. Mar. Sci. Eng. 2020, vol. 8, no. 3(200), doi: 10.3390/jmse8030200.

14. I. Asimakopoulos, L. Avendaño-Valencia, M. Lützen and N. Rytter, "Data-driven condition monitoring of two-stroke marine diesel engine piston rings with machine learning," Ships and Offshore Structures. 2023, doi: 10.1080/17445302.2023.2237302.

15. O. Bondarenko and T. Fukuda, "Development of a diesel engine's digital twin for predicting propulsion system dynamics," Energy. 2020, vol. 196, doi:10.1016/j.energy.2020.117126.

16. R. Varbanets, O. Fomin, V. Píštěk, V. Klymenko, D. Minchev, A. Khrulev, V. Zalozh and P. Kučera, "Acoustic method for estimation of marine low-speed engine turbocharger parameters," Journal of Marine Science and Engineering. 2021, vol. 3, no. 9, doi: 10.3390/jmse9030321.

17. R. Varbanets, O. Shumylo, A. Marchenko, D. Minchev, V. Kyrnats, V. Zalozh, N. Aleksandrovska, R. Brusnyk and K. Volovyk, "Concept of vibroacoustic diagnostics of the fuel injection and electronic cylinder lubrication systems of marine diesel engines," Polish Maritime Research. 2022, vol. 29, no. 4, pp. 88-96, doi: 10.2478/pomr-2022-0046.

18. S. Neumann, R. Varbanets, D. Minchev, V. Malchevsky and V. Zalozh, "Vibrodiagnostics of marine diesel engines in IMES GmbH systems," Ships and Offshore Structures. 2022, doi: 10.1080/17445302.2022.2128558.

19. O. Yeryganov and R. Varbanets, "Features of the fastest pressure growth point during compression stroke," Diagnostyka. 2018, vol. 19, no. 2, pp. 71-76, doi: 10.29354/diag/89729.

20. D. Minchev, R. Varbanets, N. Alexandrovskaya and L. Pisintsaly, "Marine diesel engines operating cycle simulation for diagnostics issues," Acta Polytechnica. 2021, vol. 61, no. 3, pp. 428-440, doi: 10.14311/ap.2021.61.0435.

21. D. Minchev, O. Gogorenko, R. Varbanets, Y. Moshentsev, V. Píštěk, P. Kučera, O. Shumylo and V. Kyrnats, "Prediction of centrifugal compressor instabilities for internal combustion engines operating cycle simulation," Proceedings of the Institution of Mechanical Engineers, Part D: Journal of

Automobile Engineering. 2023, vol. 237, no. 2-3, pp. 572-584, doi: 10.1177/09544070221075419.

22. Н. Ф. Разлейцев, Моделирование и оптимизация процесса сгорания в дизелях, Харьков: Вища школа, 1980, p. 169.

23. А. Ф. Шеховцов, Ф. И. Абрамчук and В. И. и. д. Крутов, Процессы в перспективных дизелях, Харьков: Основа, 1992, p. 352.

24. L. Grekhov, K. Mahkamov and A. Kuleshov, "Optimization of Mixture Formation and Combustion in Two-Stroke OP Engine Using Innovative Diesel Spray Combustion Model and Fuel System Simulation Software," SAE. 2015, 2015-01-1859, doi: 10.4271/2015-01-1859.

25. A. Kuleshov, K. Mahkamov, A. Kozlov and Y. Fadeev, "Simulation of dual-fuel diesel combustion with multi-zone fuel spray combustion model," Proceedings of the ASME 2014 Internal Combustion Engine Division Fall Technical Conference. 2014, pp. 1-13, doi: 10.1115/ICEF2014-5700.